ACS APPLIED ENERGY MATERIALS

www.acsaem.org Article

Strong Coupling of CdSe Quantum Dots to Single-Walled Carbon Nanotubes

Published as part of ACS Applied Energy Materials special issue "Photocatalysis"

Mengyao Bao, Facheng Guo, Seyla Azoz, Nebojsa S. Marinkovic, Matthew Y. Sfeir, Yulian He,* Victor S. Batista,* and Lisa D. Pfefferle*

Cite This: https://doi.org/10.1021/acsaem.6c01275 Read Online

ACCESS | Metrics & More | Article Recommendations | Supporting Information

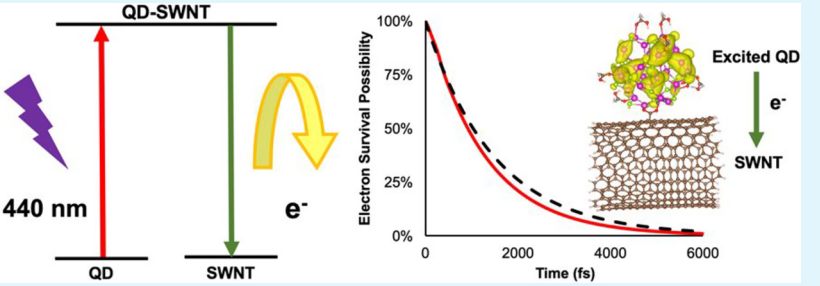

ABSTRACT: Quantum dots (QDs) and single-walled carbon nanotubes (SWNTs) have electronic and photonic properties ideally suited for applications to solar cells, catalysts, sensors, and light-emitting diodes. Many of those applications require efficient energy transfer interfacing different semiconductor nanomaterials. In this study, we develop covalently bonded interfaces to optimize charge transfer from the photoexcited QD to the carbon nanotube acceptor exploiting interfacial strong electronic coupling. Ultrafast transient absorption spectroscopy of CdSe QDs reveals considerably shorter lifetimes of electronic excited states when the QDs are covalently bonded to mildly oxidized SWNTs with surface-anchoring carboxylic acid groups. We define a set of spectroscopic fingerprints to characterize strong coupling. These include suppression of photoluminescence (PL), broadened UV-vis spectra, and transient absorption time scales faster than the picosecond timescale. Thus, the QD-SWNT assemblies were characterized by UV-visible spectroscopy, transmission electron microscopy (TEM), X-ray absorption fine structure (EXAFS), transient absorption, and photoluminescence (PL) experiments. Calculations of fully atomistic models relaxed at the density functional theory (DFT) level of theory provide a rigorous interpretation of the experiments as directly compared to the simulated Cd-edge EXAFS spectra and quantum dynamics simulations of interfacial electron transfer (IET). Charge-separated states exhibit ultrafast electron transfer from the CdSe QDs to the SWNTs due to the strong electronic coupling with negligible energy barriers for charge transport between components in the QD-SWNT nanocomposites. The experimental and theoretical calculation results consistently indicate that strong interfacial coupling fundamentally modifies the electronic structure and charge-transfer dynamics, demonstrating that the QD-SWNT assemblies cannot be regarded as a simple combination but instead a hybrid system with distinct properties.

KEYWORDS: *CdSe quantum dots, ultrafast interfacial charge transfer, single-walled carbon nanotubes, transient absorption spectroscopy, quantum dynamics simulations*

■ INTRODUCTION

Semiconductor nanocrystal quantum dots (QD) have been widely used in solar cells, photocatalysis, biological imaging, and other fields due to their adjustable band structure and controllable emission spectrum.[1−3] Meanwhile, single-walled carbon nanotubes, owing to their small dimensions, high aspect ratios, high current-carrying capacities, and ballistic transport properties, exhibit great potential in optoelectronic conversion devices.[4,5] Integrating quantum dots with single-walled carbon nanotubes (SWNTs) is expected to make full use of their characteristics to achieve efficient light absorption and fast charge transfer, thus improving the performance of

Received: April 15, 2026
Revised: June 2, 2026
Accepted: June 3, 2026

optoelectronic devices. Studies of QD-SWNT structures, like QD-pyrene-NT hybrid systems[6] and QD-NT-polymer hybrids systems,[7] have shown that engineering the QD-SWNT coupling can be critical for photoconversion by significantly improving the efficiency of charge transfer between components.[8,9] How to improve the ability to transport carriers in quantum dots while maintaining optical properties has long been a focus of scientific research. Common strategies include[10] (1) modifying the surface of quantum dots through physical methods such as ligand exchange or thermal annealing[11,12] and (2) coupling quantum dots with one-dimensional nanostructures, such as single-walled carbon nanotubes[6] or nanowires.[2] Studies have shown that the electron transfer rate typically decays exponentially with the distance between the QD donor and acceptor.[13] For a linker about 1 nm in length, the charge transfer rate is usually on the nanosecond to tens-of-nanoseconds timescale.[14,15] Additionally, the interfacial electron transfer (IET) is also dependent on the specific chemical identity of the molecular links.[14]

Compared with linker ligands, direct coupling QDs with SWNTs can significantly enhance the electron transfer rate and improve structural stability. However, the interfacial electronic coupling in the existing QD-SWNT composite systems is often difficult to evaluate accurately. Many studies have analyzed coupling simply through the performance enhancement of a catalytic process or device;[16−18] some have shown moderate suppression of photoluminescence (PL),[19,20] but little has confirmed ultrafast charge transport on the sub ns time scale by a direct probe. Although PL quenching is a common coupling diagnostic method, its signal is easily disturbed by impurity states and unbonded QDs, making it difficult to directly reflect the actual charge transfer efficiency. In addition, most of the reported systems rely on molecular linkers to achieve assembly, which may introduce additional energy barriers to hinder the rapid transport of electrons at the interface,[21] although the composite stability can be improved to some extent. For the structural characteristics and electron transfer process of strong coupling systems, there is still a lack of systematic experimental and theoretical verification.

In this study, a direct covalent bonding strategy without molecular linkers is proposed to form a tight interface between CdSe QDs and SWNTs to minimize the potential barrier of electron transport and inhibit electron-hole recombination, which can be applied to the design of electronic devices, realizing ultrafast charge transfer at the subpicosecond level. Here, we focus on understanding ultrafast charge separation at CdSe-SWNT nanocomposite interfaces. We characterize the mechanism of IET by ultrafast transient absorption (TA) measurements and validate the results with fully atomistic quantum dynamics simulations. We find that strongly coupled composite materials behave as new materials showing distinct properties relative to those of the constituent components.

We anticipate that the reported findings will have significant implications for a wide range of applications, such as solar cells where photoinduced charge transport across the nanocomposite interfaces could be critical for the device performance. The reported characterization is also expected to be valuable for studies of a wide range of interfaces of nanomaterial composites involving 2D structures, different types of nanotubes and nanowires, and a host of other geometries.

METHODS

Pretreatment of SWNTs

Acid-functionalized SWNTs were purchased from Carbon Solutions, Inc. (Riverside, CA, batch number P3-SWNT, >90% purity, 1 ± 0.5 μm length, nitric-acid-purified SWNTs containing 1.0−3.0% carboxylic acid groups as provided from the manufacturer) and further purified by HCl treatment (100 mg SWNTs refluxed with 37% HCl at 60°C overnight) to remove the metal catalysts and carbonaceous impurities. Through previous characterization, we found that this batch of SWNTs after treatments comprised the (12,10) chirality as one of the major components.[22]

CdSe QDs Synthesis

CdSe QDs were synthesized by the hot-injection colloidal route. For a typical experiment, 13 mg CdO were dissolved in 100 mL of octadecene (ODE) with the presence of 0.537 mg of oleic acid. The cadmium solution was then stirred and heated up to 225°C. At this temperature, the pre-prepared selenium solution (30 mg of Se powder, 0.4 mL of trioctylphosphine (TOP) dissolved in 10 mL of ODE) was injected quickly into the cadmium solution and was allowed to react. The samples were then collected and purified by extraction and centrifugation. Extraction was performed in a methanol/hexane mixture and the precipitation of the CdSe QDs was achieved by the centrifugation of the CdSe QDs dissolved in hexane with an excess of ethanol.

CdSe QD-SWNT Attachment

The attachment of CdSe QDs and SWNTs was performed by probe ultrasonication. A 1:1 weight ratio of CdSe QDs and SWNTs was used. SWNTs were directly dispersed in a 40 mL CdSe QD solution prepared with hexane. Probe ultrasonication (50 W power) was carried out for 2 h in an ice bath. The solution was filtered, and the QD-SWNT heterostructure was then washed 3 times, each time with 50 mL of hexane, and then oven dried at 80 °C overnight. Once the sample was dry, the powder was re-dispersed in a clean hexane solvent and used for further characterization.

Computational Methods

Structural optimizations, in this study, were performed using the quantum mechanics/molecular mechanics (QM/MM) hybrid model, where the QM region was treated at the ωB97X-D/def2-SVP level[23−25] of theory using the Gaussian 09 program,[26] and the MM region was described by the UFF force field.[27] The model system consisted of a $Cd_{33}Se_{33}$ quantum dot (Figure S2) covalently bonded to a fragment of a (12,10) single-walled carbon nanotube through bridged oxygen atoms (Figure S3).[28] Interfacial electron transfer (IET, Figure S4 and Section S3) was independently simulated using an Ehrenfest quantum dynamics approach based on a tight-binding extended Hückel Hamiltonian,[29−32] as implemented in the YAeHMOP program.[33] Local density of states and electronic couplings were extracted from the level-aligned Hamiltonian matrix,[34] with the initial excitation localized on the LUMO+40 orbital of the QD. More modeling details can

https://doi.org/10.1021/acsaem.6c01275
ACS Appl. Energy Mater. XXXX, XXX, XXX−XXX

be found in Sections S2 and S3 in the supplementary information.

RESULTS AND DISCUSSION

We first prepared covalently tight-bonded CdSe QDs and SWCNTs via the carboxylate anchoring strategy developed in our previous work with detailed descriptions and characterizations.[35] Briefly, during the reaction under ultrasonication, capping oleic acid (OA) ligands on the CdSe QDs were exchanged by carboxylate groups from the SWNTs, establishing covalent binding of the SWNTs to Cd centers on the CdSe surface, as confirmed from our previous work.[35] This covalent bonding facilitates strong interfacial coupling between the CdSe QDs and SWNTs (vide infra).[18] The structure of CdSe QD-SWNT nanocomposites was first confirmed with high-resolution transmission electron microscopy (TEM). Figures 1a and S1 confirm a uniform distribution of CdSe QDs, with an intact average size of 3.05 ± 0.25 nm in diameter, over SWNTs to form QD-SWNT composite. A schematic illustration for the ligand exchange process is shown in Figure 1b. Here, this covalent bonding is also suggested by our experimental EXAFS data at the Cd K edge for pure CdSe QDs (Figure 1c) and QD-SWNT (Figure 1d). First of all, the similarity between the EXAFS spectra of CdSe QDs and CdSe-SWNTs suggests that the structure of the CdSe QDs was largely preserved upon the formation of the nanocomposite, while variations can still be found at the lower radial distance regions. As shown in Figure S6a,b, bulk CdSe shows a single peak at ∼2.6 Å, corresponding to the Se neighbors in the first coordination shell of Cd.[36] In contrast, the CdSe QDs counterpart shows an additional peak at ∼2.3 Å due to the interaction between CdSe and the capping OA agent.[37] Our previous experimental and theoretical analyses have ascribed this feature to be the Cd–O neighbor scattering path rather than Cd-C.[35] Importantly, upon the formation of the covalently bonded QD-SWNT, the Cd-O signal intensifies while the Cd-Se coordination decreases with the Cd-Se bond length remaining essentially unchanged (Tables S1−S3). These trends indicate that surface Cd sites of the CdSe QDs are partially converted from ligand/Se-rich local environments into Cd-O interfacial environments associated with carboxylate groups on the SWNT surface, while the CdSe core structure is largely retained. The Cd-O anchoring motif therefore provides a direct structural bridge between the QD and SWNT, reducing the interfacial tunneling distance and enabling stronger electronic coupling than linker-mediated or weakly adsorbed assemblies.[35]

To probe the electronic effects of CdSe-SWNT coupling, we first investigated their optical absorption behaviors using UV-vis spectroscopy. Figure 2 shows the UV-Vis absorption spectra of CdSe QDs, obtained before and after SWNTs attachment. On its own, CdSe QDs show a prominent absorption feature centered around 520 nm, whereas SWNTs do not absorb at all in the 400−800 nm range. Interestingly, the absorption feature of CdSe QDs has been smeared out after covalently bonding to SWNTs via the proposed ultrasonication procedure. To verify that the observed optical changes arise from covalent coupling rather than physical mixing or ultrasonic treatment, we designed a series of control experiments. First, CdSe QDs and SWNTs were physically mixed at a 1:1 ratio and magnetically stirred for 2 h without ultrasonic treatment. The resulting UV−vis absorption spectrum showed no change compared with that of CdSe QDs alone, indicating that the optical properties remained unchanged. Second, CdSe QDs alone were subjected to ultrasonic treatment; although the absorption spectrum exhibited slight broadening, the characteristic absorption peaks of CdSe QDs were retained, suggesting that ultrasonication itself does not significantly affect their structure. These results indicate that changes occurred between CdSe QDs and SWNTs in ultrasonication differ from those in simple physical mixing. Combined with the EXAFS data, we reasonably attribute this to effective covalent coupling between the quantum dots and SWNTs, which disturb their excited-state distribution.

Additionally, normalized photoluminescence (PL) spectra also confirmed a strong electronic interaction between CdSe QDs and SWNTs upon covalent bonding. As shown in Figure 3, the fluorescence intensity (i.e., excitonic emission) of CdSe QDs is significantly quenched after binding with SWNTs, with a quenching efficiency exceeding 99%. The result indicates that there is a strong electronic coupling between CdSe QDs and SWNTs, leading to an alternative charge transfer from CdSe QDs to SWNTs instead of the excitonic emission.[38] Theoretically, the charge transfer can occur in three possible pathways: hole transfers, electron transfers, or both.[38,39] Since carbon nanotubes are known for high electron affinities,[10,15] we posit the dominant mechanism is most likely to be the electron transfer from the conduction band of CdSe QDs to the electron acceptor states in SWNTs.[35]

Direct attachment reduces the distance between the electron donor and acceptor units, allowing efficient transfer of electrons or holes across the interfaces, either through the anchoring group or by tunneling.[40] Although PL measurements support the occurrence of electron transfer by showing emission quenching, they only reflect the minority of emissive species in the sample. As a result, the spectra can be dominated by impurities or unbound QDs, limiting the reliability of PL in capturing overall charge transfer dynamics. Therefore, we employed transient absorption (TA) spectroscopy (Figure 4), which captures the majority of the species within the sample and is more reflective of the overall charge transfer processes by giving information about the evolution of nonemissive decay processes and dark states.

We employed ultrafast pump-probe laser spectroscopy to probe the photoinduced charge transfer processes since the interfacial electron transfer in the CdSe-SWNT assembly would likely occur in the sub-picosecond to picosecond time scale.[41−43] We monitored temporal changes in absorbance following laser pulse pumping at both 440 nm (2.81 eV, slightly larger than the 2.30 eV band gap of 3 nm CdSe QD)[44] and 700 nm, above and below the first excitonic peak of CdSe (∼550 nm), to monitor changes in both CdSe QDs and SWNTs induced by photoexcitation. The samples were dispersed in hexane at the same concentration and diluted to achieve optimal optical density. The batch of SWNTs and the final SWNTs concentration were kept the same to avoid changes in the TA spectra that are not due to the CdSe QDs attachment.

As shown in Figures 4 and S7, the transient spectral characteristics of CdSe-SWNTs are significantly different from those of pure SWNTs and unbound CdSe QDs, especially when the excitation energy is above or below the onset of CdSe absorption (in the 550−650 nm range and beyond 800 nm) (Figure S8). In the 550−650 nm range and above 800 nm, the negative signal (red) observed in SWNTs is converted into the positive signal (blue) upon coupling with CdSe QDs. The

https://doi.org/10.1021/acsaem.6c01275
ACS Appl. Energy Mater. XXXX, XXX, XXX−XXX

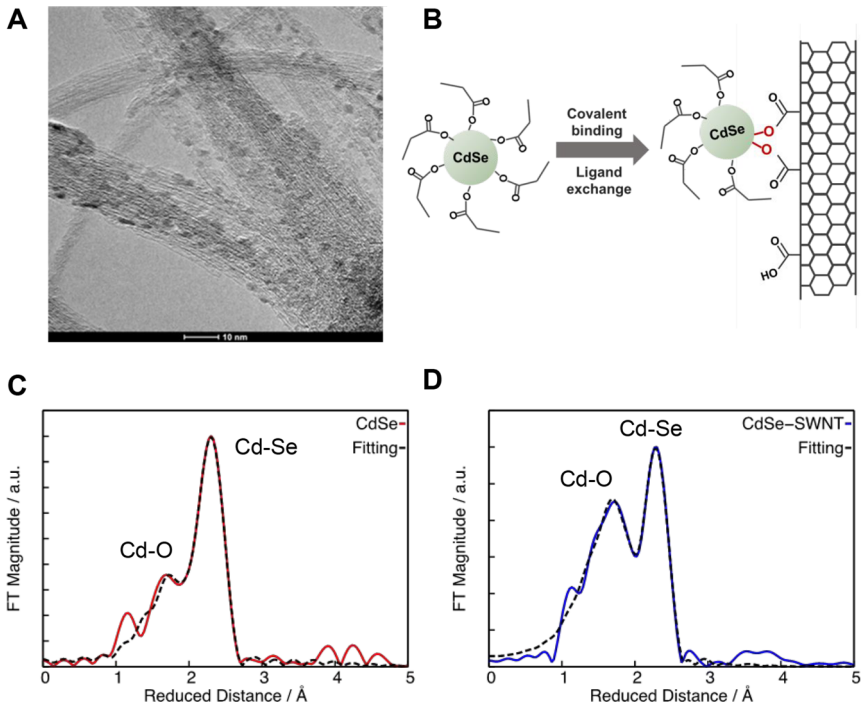

Figure 1. (a) TEM image of the CdSe QD-SWNT nanocomposite material, (b) schematic illustration of the ligand exchange process for anchoring CdSe QDs onto the SWNT. (c) Radial structure distribution functions of Cd obtained by Fourier transform of the k^2 weighted EXAFS functions (not phase corrected) for the pure CdSe QD, and (d) CdSe-SWNT composite, both fitted with CdSe and CdO.

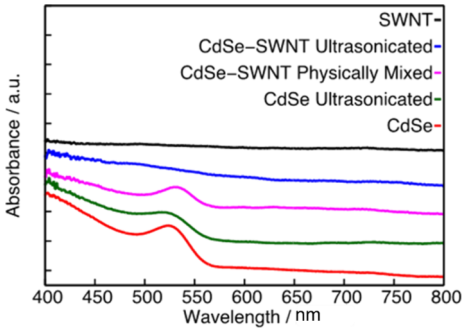

Figure 2. UV−Vis spectra of pure CdSe QDs (red), pure SWNTs (black), CdSe QDs sonicated in the absence of SWNTs (green), CdSe QDs physically mixed with SWNTs (magenta), and CdSe QDs covalently attached to SWNTs via ultrasonication (blue). The spectra are offset from each other to facilitate the comparison.

negative ΔA signal of the pristine SWNTs mainly reflects ground-state bleaching of the nanotube excitonic transitions. After CdSe QDs are covalently attached, the signal in the same spectral region becomes positive, indicating that photoinduced absorption and/or carrier-induced absorption associated with newly accessible coupled electronic states dominates over the original bleaching response. The bleaching signal in the 650−800 nm range remains visible in CdSe-SWNTs but is superimposed on a higher background, indicating photoinduced absorption arising from additional electronic interactions introduced by the CdSe QDs. Although the ground-state bleaching signal of CdSe QDs could not be directly observed (Figure S7), their attachment to SWNTs significantly change the spectral profiles of SWNTs under both excitation wavelengths, indicating strong electronic coupling between the CdSe QDs and SWNTs.

In QD-SWNTs, signatures of the CdSe exciton absorption are absent in both linear (UV-vis absorption spectroscopy, Figure 2) and transient optical measurements (Figure 4), suggesting the formation of distinct electronic states due to the strong binding between the CdSe QDs and the SWNTs. In the limit of weak coupling, 440 nm excitation should produce signals that could be approximately described by a linear combination of the individual components, while the 700 nm excitation should reproduce the unmodified SWNTs dynamics. In contrast, we find that it is not possible to isolate the individual components using selective excitation (Figure 4), suggesting the formation of a strongly coupled nanocomposite material. Both the 440 nm (where the QDs absorbs) and the 700 nm pump excitation wavelengths (where the SWNTs absorbs) produce similar responses, further suggesting formation of a strongly bound new nanocomposite. Upon attachment of CdSe QDs to SWNTs, we observe positive signals in the ΔA spectrum (Figure S8) that can be attributed to absorptive processes due to excited state absorption (transitions from the excited state to even higher excited states upon excitation with pump laser) or increase in the population of mobile electrons as new density of states become available with strong binding of CdSe QDs on SWNTs. Therefore, it is natural to conjecture that there is ultrafast electron transfer from the QDs to the strong coupled SWNTs. Although the instrument response function cannot resolve dynamics below 100 fs, the data clearly show changes in the spectra when CdSe QDs are attached to SWNTs, suggesting formation of a distinct nanocomposite material.

https://doi.org/10.1021/acsaem.6c01275
ACS Appl. Energy Mater. XXXX, XXX, XXX−XXX

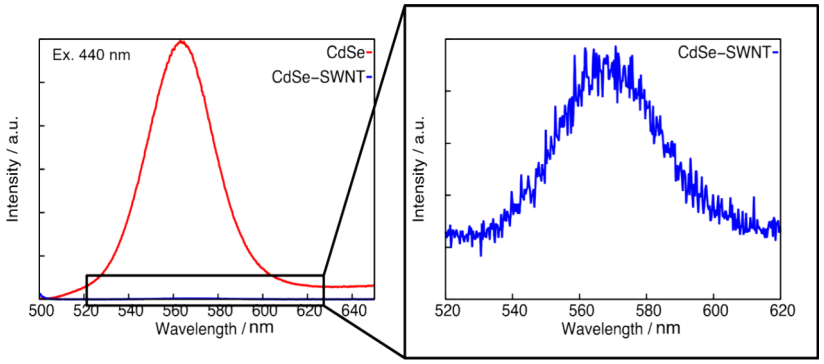

Figure 3. Left panel. Steady-state fluorescence spectra normalized to optical density at the excitation wavelengths of CdSe QDs (red) were significantly quenched upon attachment to the SWNTs (blue). The samples were dispersed in hexane at 1 mg/mL. Excitation wavelength: 440 nm. Right panel: A close-up of the QD-SWNT spectrum. The magnification of CdSe-SWNT in right plot is 300 times the scale.

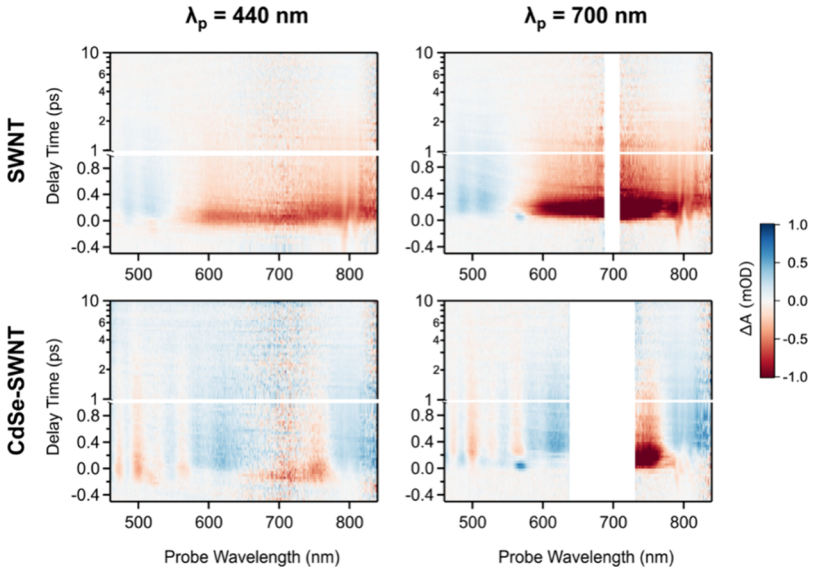

Figure 4. Transient absorption (TA) spectra of functionalized SWNTs compared to the CdSe-SWNT nanocomposite for optical excitation (λp) at 440 and 700 nm. For 700 nm optical pumping, we have removed the region where laser scatter obscures the excited state dynamics.

To quantify the time scales of the photoinduced processes, we analyzed the kinetics of the transient absorption signals. Figure 5 shows the decay profiles of transient absorption kinetics of SWNTs with and without CdSe QDs at the 800 nm probe, following 440 nm excitation. Clearly, the relaxation kinetics of the nanocomposite evolve on dramatically different time scales. For SWNTs, the signal is negative (net bleach) and evolves with two primary components (Table 1) determined from fitting to a biexponential decay (eq 1) convoluted with the instrument response, a faster decay of 0.14 ps comparable to our experimental time resolution, and a weaker secondary component that decays in 1.21 ps. In contrast, the CdSe-SWNT nanocomposite exhibits a positive signal (net absorption), attributed to electronic coupling with the CdSe QDs. Here, the primary signal decays with a time constant of 1.17 ps and notably exhibits a decay process that extends to times >11 ps. No resolvable rise process is observed in the photoinduced absorption signal, indicating that the

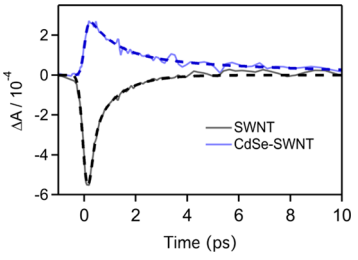

Figure 5. Decay profiles of CdSe-SWNT (top, blue) and SWNTs (bottom, black) when both solutions were pumped at 440 nm. The data are probed at 800 nm.

Table 1. Summary of Decay Constants from Bi-Exponential Fittings of the TAS Data

sample	τ_1 (ps)	τ_2 (ps)
SWNT	0.14	1.21
CdSe-SWNT	1.17	11.79

https://doi.org/10.1021/acsaem.6c01275
ACS Appl. Energy Mater. XXXX, XXX, XXX–XXX

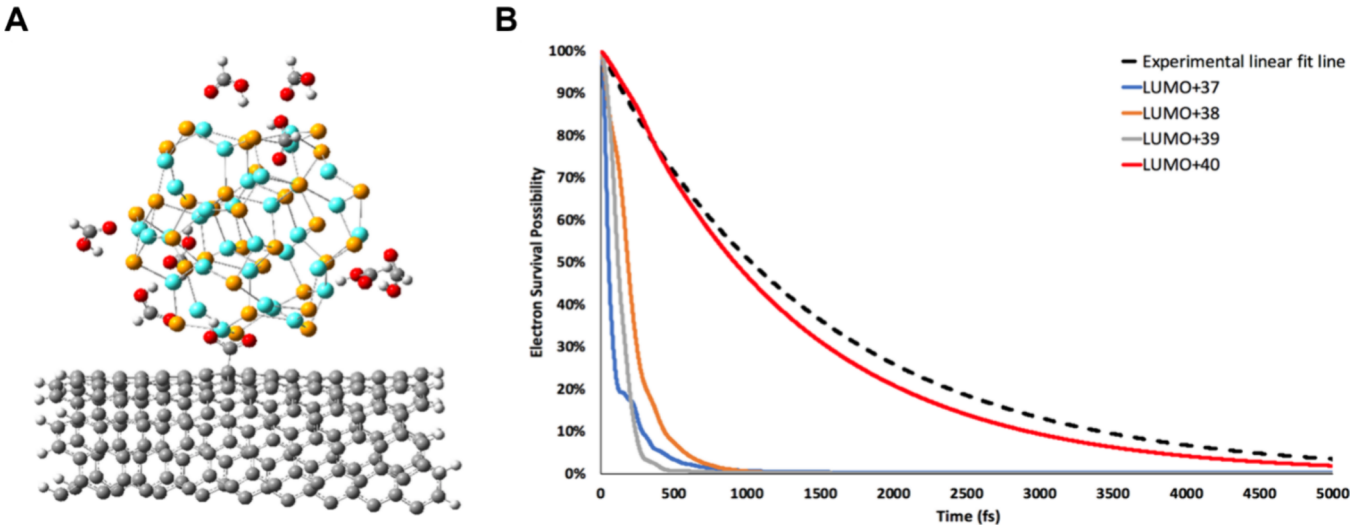

Figure 6. (a) Optimized $Cd_{33}Se_{33}$ QD-half-SWNT model obtained at the DFT level of theory, using the ωB97X-D ωB97X-D/UFF functional, The color key is as follows: teal = Cd, brown = Se, gray = C, white = H, red = O. (b) Theoretical time-dependent IET, i.e. survival probability of the electron localized on the 440 nm excited CdSe QD, of LUMO+37 (3.44 eV), LUMO+38 (3.46 eV), LUMO+39 (3.48 eV) and LUMO+40 (3.49 eV) compared with the experimental linear fit line (black dashed line). LUMO+41 (4.69 eV) and beyond is not considered due to the significantly higher energy level.

charge-separated state is formed almost instantaneously, consistent with the scenario of direct electron injection from the quantum dots into the SWNTs.

$$y = y_0 + A_1 e^{-x/\tau_1} + A_2 e^{-x/\tau_2} \quad (1)$$

The transient data will necessarily reflect the characteristic absorptions of either the weak or strong coupling situation. Here, our transient absorption data of the composite differ significantly from a simple linear combination of the individual components. As in the linear absorption, the transient spectral features in the weak coupling limit will retain the character of the individual components, although the kinetics (rate constants) will be modified due to energy and charge transfer processes. Our TA data (Figure 4 and Table 1) for the composites do not reflect this situation. Rather, our TA data are notable for the absence of the characteristic spectral features of the fundamental excitonic optical transition for the semiconductor QDs. Furthermore, the nature of the fundamental excitation characteristic of the nanotubes changes considerably by switching sign over the characteristic absorption region. This shift indicates a change in the sign of nonlinear polarization, which can only result from a significant change in the structure and occupation of the electronic energy levels. The calculations support these assertions (vide infra).

According to our simulations (Figure 6a) of interfacial electron transfer at the DFT-QM/MM level of theory (see details in Section S3), such a process would be possible since QDs are bonded directly to the SWNTs.[35] In fact, our simulations of IET by Ehrenfest quantum dynamics using a tight-binding extended-Hückel (EH) model Hamiltonian confirm ultrafast electron transfer between the excited QDs and SWNTs. The interfacial electron transfer process is complete within 500 fs when an electron is excited by 3.48 eV (up to LUMO+39). As discussed in the methods again, new material reproduces the experimental TA results, indicating ultrafast electron transfer between the covalently bonded QD-SWNT nanocomposite. The simulations used the bonding as characterized by the EXAFs results.

■ CONCLUSIONS

In this work, we have developed a direct covalent bonding strategy to assemble CdSe QDs with carboxylate-functionalized single-walled carbon nanotubes, eliminating molecular linkers. TEM, EXAFS, and DFT-QM/MM modeling confirm the bonding configuration, while >99% PL quenching, pronounced UV-vis broadening, and transient absorption (TA) spectral changes provide clear evidence of strong electronic coupling. Ultrafast TA spectroscopy combined with quantum dynamics simulations reveals sub-picosecond interfacial electron transfer from CdSe QDs to SWNTs. The experimental and theoretical results reveal that the QD-SWNT assemblies are not merely a simple combination of two individual components but rather represent a new system with a fundamentally altered electronic structure. This work not only elucidates the mechanism of ultrafast charge separation in strongly coupled nanocomposites but also offers a generalizable strategy for enhancing carrier transport in next-generation optoelectronic, photocatalytic, and quantum devices.

■ ASSOCIATED CONTENT

Supporting Information

The Supporting Information is available free of charge at https://pubs.acs.org/doi/10.1021/acsaem.6c01275.

Detailed characterization methods, additional explanation of modeling and simulation, EH parameters for CdSe, DFT calculations of bulk CdSe, additional transient absorption data, additional EXAFS data, and coordinates for the optimized QD-SWNT nanocomposite (DOCX)

https://doi.org/10.1021/acsaem.6c01275
ACS Appl. Energy Mater. XXXX, XXX, XXX–XXX

AUTHOR INFORMATION

Corresponding Authors

Yulian He – *Global College, Shanghai Jiao Tong University, Shanghai 200240, China; Department of Chemistry and Chemical Engineering, Shanghai Jiao Tong University, Shanghai 200240, China;* orcid.org/0000-0002-8994-1979; Email: yulian.he@sjtu.edu.cn

Victor S. Batista – *Department of Chemistry, Yale University, New Haven, CT 06520, USA; Energy Sciences Institute, Yale University, West Haven, CT 06516, USA;* orcid.org/0000-0002-3262-1237; Email: victor.batista@yale.edu

Lisa D. Pfefferle – *Department of Chemical and Environmental Engineering, Yale University, New Haven, CT 06520, USA;* Email: lisa.pfefferle@yale.edu

Authors

Mengyao Bao – *Global College, Shanghai Jiao Tong University, Shanghai 200240, China*

Facheng Guo – *Department of Chemistry, Yale University, New Haven, CT 06520, USA*

Seyla Azoz – *Department of Chemical and Environmental Engineering, Yale University, New Haven, CT 06520, USA*

Nebojsa S. Marinkovic – *Photonics Initiative, Advanced Science Research Center, City University of New York, New York, NY 10031, USA;* orcid.org/0000-0003-3579-3453

Matthew Y. Sfeir – *Department of Physics, Graduate Center, City University of New York, New York, NY 10016, USA*

Complete contact information is available at: https://pubs.acs.org/doi/10.1021/acsaem.6c01275

Notes

The authors declare no competing financial interest.

ACKNOWLEDGMENTS

Y.H. would like to thank the National Key R&D Program of China (2024YFA1509901) for the financial support. V.S.B. acknowledges funding from the Center for Light Energy Activated Redox Processes (LEAP), an Energy Frontier Research Center funded by the U.S. Department of Energy, Office of Science, Office of Basic Energy Sciences under Award Numbers DE-PS02-08ER15944. V.S.B. also acknowledges high-performance computing time from NERSC and from the Yale University Faculty of Arts and Sciences High Performance Computing Center, whose acquisition was partially funded by the National Science Foundation under grant number CNS08-21132. S.A. and L.D.P. would like to graciously thank the generous support of Army Research Office for funding this research under ARO grant No. W911NF2210249 and would like to thank the YINQE and CRISP facilities for providing access to assistance with TEM, SEM, and XRD instruments. The authors thank Drs. Benjamin Rudshteyn, Mikhail Askerka for Wendu Ding, Ke Yang, Adam Matula, and Svante Hedström for their advice and discussion on the theoretical calculations. The authors thank Dr. Fang Ren for EXAFS measurement. The authors thank Prof. Danny Frederickson (University of Wisconsin at Madison) for providing his *eHtuner.c* program as well as CdSe parameters generated with it. This research used resources of the Center for Functional Nanomaterials, which is a U.S. DOE Office of Science Facility, at Brookhaven National Laboratory under Contract No. DE-SC0012704.

REFERENCES

(1) Coe, S.; Woo, W.-K.; Bawendi, M.; Bulović, V. Electroluminescence from Single Monolayers of Nanocrystals in Molecular Organic Devices. *Nature* **2002**, *420* (6917), 800–803.

(2) Huynh, W. U.; Peng, X.; Alivisatos, A. P. CdSe Nanocrystal Rods/Poly(3-Hexylthiophene) Composite Photovoltaic Devices. *Adv. Mater.* **1999**, *11* (11), 923–927.

(3) Konstantatos, G.; Howard, I.; Fischer, A.; Hoogland, S.; Clifford, J.; Klem, E.; Levina, L.; Sargent, E. H. Ultrasensitive Solution-Cast Quantum Dot Photodetectors. *Nature* **2006**, *442* (7099), 180–183.

(4) Soavi, G.; Scotognella, F.; Lanzani, G.; Cerullo, G. Ultrafast Photophysics of Single-Walled Carbon Nanotubes. *Adv. Opt. Mater.* **2016**, *4* (11), 1670–1688.

(5) Blackburn, J. L. Semiconducting Single-Walled Carbon Nanotubes in Solar Energy Harvesting. *ACS Energy Lett.* **2017**, *2* (7), 1598–1613.

(6) Hu, L.; Zhao, Y.-L.; Ryu, K.; Zhou, C.; Stoddart, J. F.; Grüner, G. Light-Induced Charge Transfer in Pyrene/CdSe-SWNT Hybrids. *Adv. Mater.* **2008**, *20* (5), 939–946.

(7) Raffaelle, R. P.; Landi, B. J.; Evans, C. M.; Castro, S. L.; Bailey, S. G. Quantum Dot-Single Wall Carbon Nanotube Complexes for Polymeric Solar Cells. In *Conference Record of the Thirty-first IEEE Photovoltaic Specialists Conference, 2005*; Institute of Electrical and Electronics Engineers, **2005**; pp 74–77.

(8) Peng, X.; Sfeir, M. Y.; Zhang, F.; Misewich, J. A.; Wong, S. S. Covalent Synthesis and Optical Characterization of Double-Walled Carbon Nanotube−Nanocrystal Heterostructures. *J. Phys. Chem. C* **2010**, *114* (19), 8766–8773.

(9) Bang, J. H.; Kamat, P. V. CdSe Quantum Dot–Fullerene Hybrid Nanocomposite for Solar Energy Conversion: Electron Transfer and Photoelectrochemistry. *ACS Nano* **2011**, *5* (12), 9421–9427.

(10) Jeong, S.; Shim, H. C.; Kim, S.; Han, C.-S. Efficient Electron Transfer in Functional Assemblies of Pyridine-Modified NQDs on SWNTs. *ACS Nano* **2010**, *4* (1), 324–330.

(11) Yu, D.; Wang, C.; Guyot-Sionnest, P. N-Type Conducting CdSe Nanocrystal Solids. *Science* **2003**, *300* (5623), 1277–1280.

(12) Jarosz, M. V.; Porter, V. J.; Fisher, B. R.; Kastner, M. A.; Bawendi, M. G. Photoconductivity Studies of Treated CdSe Quantum Dot Films Exhibiting Increased Exciton Ionization Efficiency. *Phys. Rev. B* **2004**, *70* (19), 195327.

(13) Marcus, R. A. On the Theory of Electron-Transfer Reactions. VI. Unified Treatment for Homogeneous and Electrode Reactions. *J. Chem. Phys.* **1965**, *43* (2), 679–701.

(14) Hu, L.; Zhao, Y.; Ryu, K.; Zhou, C.; Stoddart, J. F.; Grüner, G. Light-Induced Charge Transfer in Pyrene/CdSe-SWNT Hybrids. *Adv. Mater.* **2008**, *20*, 939.

(15) Wang, L.; Han, J.; Sundahl, B.; Thornton, S.; Zhu, Y.; Zhou, R.; Jaye, C.; Liu, H.; Li, Z.-Q.; Taylor, G. T.; Fischer, D. A.; Appenzeller, J.; Harrison, R. J.; Wong, S. S. Ligand-Induced Dependence of Charge Transfer in Nanotube–Quantum Dot Heterostructures. *Nanoscale* **2016**, *8* (34), 15553–15570.

(16) Han, X.; Wu, X.; Zhong, C.; Deng, Y.; Zhao, N.; Hu, W. $NiCo_2S_4$ Nanocrystals Anchored on Nitrogen-Doped Carbon Nanotubes as a Highly Efficient Bifunctional Electrocatalyst for Rechargeable Zinc-Air Batteries. *Nano Energy* **2017**, *31*, 541–550.

(17) Liao, T.; Sun, Z.; Sun, C.; Dou, S. X.; Searles, D. J. Electronic Coupling and Catalytic Effect on H_2 Evolution of MoS_2/Graphene Nanocatalyst. *Sci. Rep.* **2014**, *4* (1), 6256.

(18) Liang, Y.; Li, Y.; Wang, H.; Dai, H. Strongly Coupled Inorganic/Nanocarbon Hybrid Materials for Advanced Electrocatalysis. *J. Am. Chem. Soc.* **2013**, *135* (6), 2013–2036.

(19) Biju, V.; Itoh, T.; Baba, Y.; Ishikawa, M. Quenching of Photoluminescence in Conjugates of Quantum Dots and Single-Walled Carbon Nanotube. *J. Phys. Chem. B* **2006**, *110* (51), 26068–26074.

(20) Attanzio, A.; Sapelkin, A.; Gesuele, F.;van der Zande, A.; Gillin, W. P.; Zheng, M.; Palma, M. Carbon Nanotube-Quantum Dot Nanohybrids: Coupling with Single-Particle Control in Aqueous Solution. *Small* **2017**, *13* (16), 1603042.
(21) Peng, X.; Misewich, J. A.; Wong, S. S.; Sfeir, M. Y. Efficient Charge Separation in Multidimensional Nanohybrids. *Nano Lett.* **2011**, *11* (11), 4562–4568.
(22) Ravel, B.; Newville, M. ATHENA, ARTEMIS, HEPHAESTUS: Data Analysis for X-Ray Absorption Spectroscopy Using IFEFFIT. *J. Synchrotron Rad.* **2005**, *12* (4), 537–541.
(23) Weigend, F. Accurate Coulomb-Fitting Basis Sets for H to Rn. *Phys. Chem. Chem. Phys.* **2006**, *8* (9), 1057–1065.
(24) Weigend, F.; Ahlrichs, R. Balanced Basis Sets of Split Valence, Triple Zeta Valence and Quadruple Zeta Valence Quality for H to Rn: Design and Assessment of Accuracy. *Phys. Chem. Chem. Phys.* **2005**, *7* (18), 3297–3305.
(25) Chai, J.-D.; Head-Gordon, M. Long-Range Corrected Hybrid Density Functionals with Damped Atom–Atom Dispersion Corrections. *Phys. Chem. Chem. Phys.* **2008**, *10* (44), 6615–6620.
(26) Frisch, M. J.; Trucks, G. W.; Schlegel, H. B.; Scuseria, G. E.; Robb, M. A.; Cheeseman, J. R.; Scalmani, G.; Barone, V.; Mennucci, B.; Petersson, G. A.; Nakatsuji, H.; Caricato, M.; et al. *Gaussian 09, Revision D.01*; Gaussian, Inc.: Wallingford, CT, **2009**.
(27) Rappe, A. K.; Casewit, C. J.; Colwell, K. S.; Goddard, W. A. I.; Skiff, W. M. UFF, a Full Periodic Table Force Field for Molecular Mechanics and Molecular Dynamics Simulations. *J. Am. Chem. Soc.* **1992**, *114* (25), 10024–10035.
(28) Veiga, R. G. A.; Tomanek, D.; Frederick, N. *Tube ASP: Carbon Nanotube Generation Applet*; Michigan State University. https://nanotube. msu. edu/tubeASP (accessed 2026-06-04).
(29) Rego, L. G. C.; Batista, V. S. Quantum Dynamics Simulations of Interfacial Electron Transfer in Sensitized TiO_2 Semiconductors. *J. Am. Chem. Soc.* **2003**, *125* (26), 7989–7997.
(30) Rego, L. G. C.; da Silva, R.; Freire, J. A.; Snoeberger, R. C.; Batista, V. S. Visible Light Sensitization of TiO_2 Surfaces with Alq3 Complexes. *J. Phys. Chem. C* **2010**, *114* (2), 1317–1325.
(31) Abuabara, S. G.; Rego, L. G. C.; Batista, V. S. Influence of Thermal Fluctuations on Interfacial Electron Transfer in Functionalized TiO_2 Semiconductors. *J. Am. Chem. Soc.* **2005**, *127* (51), 18234–18242.
(32) Abuabara, S. G.; Cady, C. W.; Baxter, J. B.; Schmuttenmaer, C. A.; Crabtree, R. H.; Brudvig, G. W.; Batista, V. S. Ultrafast Photooxidation of Mn(II)−Terpyridine Complexes Covalently Attached to TiO_2 Nanoparticles. *J. Phys. Chem. C* **2007**, *111* (32), 11982–11990.
(33) Landrum, G.; Glassey, W. *Yet Another Extended Ḧuckel Molecular Orbital Package (YAeHMOP) Version 3.0 User Manual*; Cornell University: Ithaca, NY, **1995**.
(34) Kienle, D.; Cerda, J. I.; Ghosh, A. W. Extended Hückel Theory for Band Structure, Chemistry, and Transport. I. Carbon Nanotubes. *J. Appl. Phys.* **2006**, *100* (4), 043714.
(35) Azoz, S.; Jiang, J.; Keskar, G.; McEnally, C.; Alkas, A.; Ren, F.; Marinkovic, N.; Haller, G. L.; Ismail-Beigi, S.; Pfefferle, L. D. Mechanism for Strong Binding of CdSe Quantum Dots to Multiwall Carbon Nanotubes for Solar Energy Harvesting. *Nanoscale* **2013**, *5* (15), 6893–6900.
(36) Bailar, J. C. *Comprehensive Inorganic Chemistry*; Elsevier, **2013**.
(37) Demchenko, I. N.; Denlinger, J. D.; Chernyshova, M.; Yu, K. M.; Speaks, D. T.; Olalde-Velasco, P.; Hemmers, O.; Walukiewicz, W.; Derkachova, A.; Lawniczak-Jablonska, K. Full Multiple Scattering Analysis of XANES at the Cd L 3 and O K Edges in CdO Films Combined with a Soft-x-Ray Emission Investigation. *Phys. Rev. B* **2010**, *82* (7), 075107.
(38) Olek, M.; Büsgen, T.; Hilgendorff, M.; Giersig, M. Quantum Dot Modified Multiwall Carbon Nanotubes. *J. Phys. Chem. B* **2006**, *110* (26), 12901–12904.
(39) Maity, P.; Debnath, T.; Chopra, U.; Ghosh, H. N. Cascading Electron and Hole Transfer Dynamics in a CdS/CdTe Core–Shell Sensitized with Bromo-Pyrogallol Red (Br-PGR): Slow Charge Recombination in Type II Regime. *Nanoscale* **2015**, *7* (6), 2698–2707.
(40) Pettersson, K.; Wiberg, J.; Ljungdahl, T.; Mårtensson, J.; Albinsson, B. Interplay between Barrier Width and Height in Electron Tunneling: Photoinduced Electron Transfer in Porphyrin-Based Donor−Bridge−Acceptor Systems. *J. Phys. Chem. A* **2006**, *110* (1), 319–326.
(41) Huang, J.; Huang, Z.; Yang, Y.; Zhu, H.; Lian, T. Multiple Exciton Dissociation in CdSe Quantum Dots by Ultrafast Electron Transfer to Adsorbed Methylene Blue. *J. Am. Chem. Soc.* **2010**, *132* (13), 4858–4864.
(42) Boulesbaa, A.; Issac, A.; Stockwell, D.; Huang, Z.; Huang, J.; Guo, J.; Lian, T. Ultrafast Charge Separation at CdS Quantum Dot/Rhodamine B Molecule Interface. *J. Am. Chem. Soc.* **2007**, *129* (49), 15132–15133.
(43) Jin, S.; Lian, T. Electron Transfer Dynamics from Single CdSe/ZnS Quantum Dots to TiO2 Nanoparticles. *Nano Lett.* **2009**, *9* (6), 2448–2454.
(44) Jasieniak, J.; Califano, M.; Watkins, S. E. Size-Dependent Valence and Conduction Band-Edge Energies of Semiconductor Nanocrystals. *ACS Nano* **2011**, *5* (7), 5888–5902.

https://doi.org/10.1021/acsaem.6c01275
ACS Appl. Energy Mater. XXXX, XXX, XXX–XXX